J. Synchrotron Rad. (1999). **6**, 618–620

Grazing-incidence XAFS studies of aqueous Zn(II) on sapphire single crystals

Thomas P. Trainor[a,*], Jeffrey P. Fitts[a], Daniel Grolimund[a], John R. Bargar[b], and Gordon E. Brown, Jr.[a,b]

[a] *Stanford University, GES, Stanford, CA 94305, USA*
[b] *Stanford Synchrotron Radiation Laboratory, SLAC, Stanford University, Stanford, CA 94309 USA.*
E-mail:trainor@pangea.stanford.edu

Grazing-incidence XAFS was applied to study the sorption of Zn(II) on two crystallographically distinct surfaces of highly polished sapphire single crystals as a simplified analog for metal ion sorption on natural aluminum-(hydr)oxides. Experiments were performed both *in-situ* (in contact with bulk solution) and *ex-situ* in a humidified N_2 atmosphere. The identification of an Al shell at roughly 3Å in all samples indicates that Zn(II) binds as an inner sphere complex on both the (0001) and (1-102) surfaces. Polarization dependence of the XAFS spectra is used to propose possible sorption species.

Keywords: Grazing Incidence XAFS; Zinc; Aluminum Oxide

1. Introduction

Sorption of dissolved metal ions on oxide surfaces plays an important role in determining the fate of metals in surface and ground waters as well as in industrial and domestic waste waters. High surface area powdered oxides are often used as sorbents in water treatment as well as for preparation of heterogeneous metal oxide on metal oxide catalysts. Therefore, an understanding of key variables affecting sorption of dissolved metals on oxide surfaces is needed for various environmental and technological applications. In particular, the role of oxide surface structure and solution conditions in determining the extent of metal ion sorption and types of sorption complexes formed could provide important information on the stability and reactivity of the sorption products.

In this study we have applied Grazing Incidence X-ray Absorption Fine Structure (GI-XAFS) spectroscopy to characterize the structure of Zn(II) sorption products on oriented single crystals of sapphire (α-Al_2O_3). Zn(II) is a common aqueous pollutant found in industrial effluent and as a product of the dissolution of mine tailings. Sapphire serves as a model substrate of commonly occurring aluminum-(hydr)oxide phases. The advantages of using single crystals in the GI-XAFS geometry include (1) well defined substrate surface, (2) ability to study polarization dependence of the sorbate species relative to the sorbent and (3) increased surface sensitivity compared to conventional powder XAFS.

2. Experimental

Highly polished single crystal α-Al_2O_3 (Union Carbide Crystal Products) substrates of the specified orientation (2" diameter) were washed in nitric acid, methanol, and multiple rinses of MilliQ water prior to equilibration with metal solutions. Samples were characterized by XPS (Surface Science S-Probe, monochromatic Al Kα radiation) prior to reaction to ensure cleanliness (estimated detection limit of zinc is 0.05 μmoles/m^2), and after reaction to estimate metal ion uptake (Table 1). Surface roughness measured by x-ray reflectivity was typically in the range of 2-5 Å RMS. Metal bearing solutions were prepared from reagent grade chemicals in a N_2-purged glove box to prevent CO_2 contamination.

Experiments were performed at the Stanford Synchrotron Radiation Laboratory (SSRL) on beamlines 6-2 and 4-2 using Si(111) or Si(220) double crystal monochromators, the SSRL grazing incidence apparatus, and a 13 element Ge array detector (Canberra). A Pt coated focusing mirror located upstream of the monochromator was used on both beam lines. The beam was slitted to roughly 150μm vertically before the Io chamber (N_2 filled ionization chamber). *In-situ* samples were mounted in a Teflon solution cell and sealed with a thin (1.5μm) polypropylene film. The cell was purged with N_2 prior to being filled with the metal bearing solution. After equilibration a negative pressure was applied to the cell to generate a thin water film over the crystal surface. The thickness of the water film (typically about 1-2μm) was characterized by x-ray reflectivity prior to collection of XAFS data. During data collection the air space above the cell was purged with humidified N_2. *Ex-situ* samples were prepared by equilibration in the metal-bearing solution in a N_2 purged glove box and maintained in a humidified (>80% r.h.) N_2 environment during data collection.

XAFS data were collected in the specular geometry with the incident angle set slightly below the critical angle of the oxide substrate (≈0.2°). Data collection was performed in both horizontal (E-vector parallel to substrate surface) and vertical (E-vector perpendicular to substrate) samples orientations. Additionally, horizontal data on the *ex-situ* α-Al_2O_3 (1-102) sample was collected with the E-vector perpendicular ($\perp$) and parallel (||) to the [-1 1 1] direction.

Data analysis was performed using EXAFSPAK (George and Pickering, 1995) with phase and amplitude functions calculated using Feff 7.0 (Rehr et al., 1991). Final fits were performed on the raw EXAFS data over the k-range of approximately 3-10 Å^{-1}. Estimated accuracy of results based on fits to model compounds for the 1st, 2nd and 3rd shells are ~ ±0.02, ±0.05 and ±0.1 Å for R and ~±10%, ±30% and ±50% for the coordination number respectively. It is noted that coordination numbers obtained from fits to polarized EXAFS data are effective coordination numbers (N_{eff}), dependent on the orientation of the polarization vector relative to the absorber-backscatterer vector (Citrin, 1985). For K-edge XAFS the largest N_{eff} results when the polarization and absorber-backscatterer vectors are parallel.

3. Results and Discussion

Solution conditions were chosen to avoid saturation with respect to hydroxides, carbonates, and basic salt precipitates (Baes and Mesmer, 1976) while obtaining sufficient metal uptake for XAFS data collection. Final solution conditions used for sample preparation were 30μM $Zn(NO_3)_2$, pH 7 with 0.01M $NaNO_3$ background electrolyte (sample D was prepared without the addition of the $NaNO_3$ electrolyte). Zn K-edge EXAFS and Fourier transforms (un-corrected for phase shift) are shown in Figure 1, and curve fitting results are given in Table 1. Analysis of the second and third shells of two representative samples is shown in Figure 2.

3.1 Ex-Situ samples

The first-shell fits of the *ex-situ* samples (A, C, D) indicate that the sorbed Zn(II) is likely six-fold coordinated by oxygen based on comparison of Zn-O distances in model compounds

Sample	Orient	Shell	N_{eff}	R(Å)	σ^2(Å^2)
A.	Al	Zn-O	6.6(9)	2.06(1)	0.011(1)
(1-102),	horz	Zn-Al	4(2)	3.09(2)	0.012(5)
ex-situ	_|_	Zn-Al	2(1)	3.70(4)	0.01*
Γ=0.2		Zn-Al	3(1)	4.08(3)	0.01*
	A2	Zn-O	7.0(6)	2.05(1)	0.0092(8)
	horz ||	Zn-Al	4.1(4)	3.04(1)	0.01*
		Zn-Al	3.0(7)	3.65(2)	0.01*
		Zn-Al	3.8(8)	4.04(2)	0.01*
	A3	Zn-O	6.0(6)	2.07(1)	0.008(1)
	vert	Zn-Al	2.3(5)	3.07(2)	0.01*
B.	B1	Zn-O	5.0(6)	1.99(1)	0.008(1)
(1-102),	horz	Zn-Al	1.5(6)	3.11(4)	0.01*
in-situ		Zn-Al	1.5(8)	3.54(4)	0.01*
Γ=1.9†	B2	Zn-O	5.8(7)	1.97(1)	0.012(2)
	vert	Zn-Al	1.8(5)	2.97(2)	0.01*
C.	C1	Zn-O	5.8(4)	2.01(1)	0.008*
(0001),	vert	Zn-Al	1.6(8)	2.90(4)	0.01*
ex-situ	C2	Zn-O	6.9(1)	2.05(1)	0.009(2)
Γ=0.3	horz	Zn-Al	5(1)	3.05(2)	0.01*
		Zn-Al	10(1)	4.06(2)	0.01*
D.	D1	Zn-O	6(1)	2.04(1)	0.010(2)
(0001),	horz	Zn-Al	3.4(7)	3.07(2)	0.008*
ex-situ		Zn-Al	7(1)	4.08(2)	0.01*
Γ=0.2					
E.	E1	Zn-O	5.5(2)	1.96(1)	0.01*
(0001),	horz	Zn-Al	2.1(6)	3.14(3)	0.01*
in-situ		Zn-Al	2.9(8)	3.56(3)	0.01*
Γ=0.3	E2	Zn-O	4.9(5)	1.99(1)	0.008(1)
	vert	Zn-Al	1.5(6)	3.04(3)	0.01*

Table 1. Curve fitting results for Zn(II)/α-Al_2O_3 samples with Al as second and third shells. See Fig. 2 for comparison with Zn in the more distant shells. Estimated errors at the 95% confidence interval are given in parenthesis. Surface coverage estimates (Γ) are given in μmoles/m^2. Equilibration times were 16 hours for samples A and C and 1 hour for samples B, D and E. * held fixed in final fit. †This high coverage number is likely a result of precipitation of Zn-nitrate salt upon removal of the sample from the *in-situ* cell.

where Zn(II) in six-fold coordination typically has Zn-O distances ≥ 2.05Å (eg. smithsonite, $Zn^{VI}CO_3$, R_{Zn-O}=2.14Å (Effenberger et al., 1981) and $Zn^{VI}(H_2O)_{6(aq)}$ R_{Zn-O}=2.05Å (Munoz-Paez et al.,1995)). Further, it appears that the first-shell is not significantly distorted due to the lack of strong polarization dependence of the first shell distance or effective coordination number. The second-shell feature is well fit by Al (Fig. 2) at approximately 2.90-3.07 Å in all cases. This range of distances is consistent with a bidentate linkage (likely edge-sharing) of Zn(II) to an AlO_6 octahedron. Comparison of the two horizontal orientations collected for the (1-102) *ex-situ* sample shows that there is little polarization dependence with respect to the [-1 1 1] direction (A1 vs. A2).

A third-shell feature is visible in the *ex-situ* horizontal orientation which is absent in the vertical orientation, suggesting that this more distant shell lies primarily in the plane of the surface. Best fits of the third shell with Al give distances of ~3.7 and 4.0 Å on the (1-102) surface (samples A1 and A2) while the (0001) horizontal spectra (C2 and D1) give an Al distance of ~4.1Å. The third shell feature is significantly stronger for the (0001) samples. An additional Al shell at ~3.6Å can be included in the fit of the (0001) horizontal spectra, however, it does not significantly improve the overall fit and only reduces the coordination number of the shell at ~4.1 Å by 30%. However, the inclusion of multiple scattering paths (e.g. Zn-O-Al) may explain the large intensity of this feature. In particluar multiple scattering from a near linear path can lead to a focusing effect resulting in large amplitudes of the multiple scattering feature (for eg. see Ressler et al., 1998). Analysis to account for multiple scattering in the data is on-going and will be presented in a future publication.

Preliminary attempts to rationalize the observed spectra with monomeric sorption geometries, assuming bulk termination of the oxide, was unsuccessful. The similiarity of the results from the two surfaces and lack of azimuthal polarization dependence on the (1-102) surface leads us to postualte one model in which sorption is occuring predominantly at step sites resulting in the strong signal from the third shell Al in the horizontal spectra. If this is the case, the higher N_{eff} for third shell Al on the (0001) may indicate a higher density of such sites on this surface.

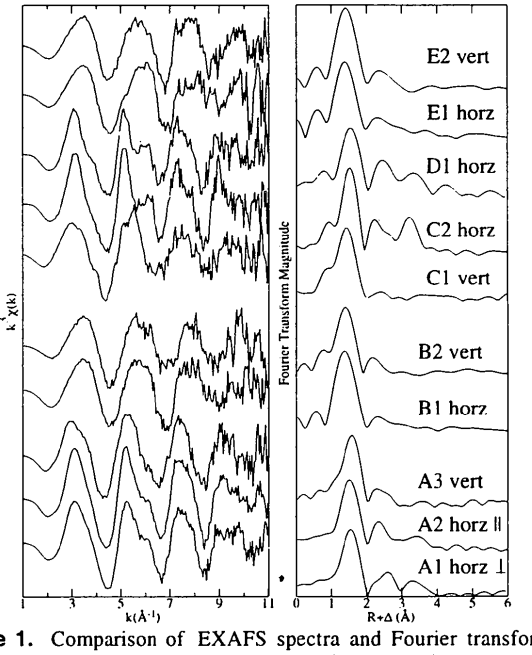

Figure 1. Comparison of EXAFS spectra and Fourier transforms (un-corrected for phase shift) for Zn(II)/α-Al_2O_3 samples.

However, as shown in Fig. 2 it is also possible to fit this more distant feature with a zinc shell at roughly 3.8Å on both surfaces. The presence of zinc in the horizontal plane may indicate the formation of oriented precipitates or zinc surface clusters/ploymerized chains. This feature is present in the sample prepared without addition of $NaNO_3$ electrolyte (D) and in a duplicate sample of (A) which was washed prior to examination (not shown). Therefore, precipitation of Zn-nitrate salts seems unlikely. In addition the 3.8Å Zn-Zn distance is longer than would be expected for a next nearest neighbor zinc based on comparison to model compounds (Fig 3) where a strong contribution from a zinc backscatterer in the range of ~3.1-3.6Å would be expected. The observed Zn-Zn distance is in the range of what might be expected for corner sharing linkage of hydroxo-bridged polymer chains and thus we cannot rule out the formation of these species.

3.2 In-Situ samples

The *in-situ* samples (B,E) have first-shell Zn-O distances (1.96-1.99 Å) in the range expected for Zn(II) in four-fold coordination. There should be some component of Zn(II) in six fold coordination convolved with these spectra due to the presence of the bulk metal solution. Inclusion of a second oxygen shell at a longer distance generally improved fits of the *in-situ* spectra; however, due to the limited range of data,

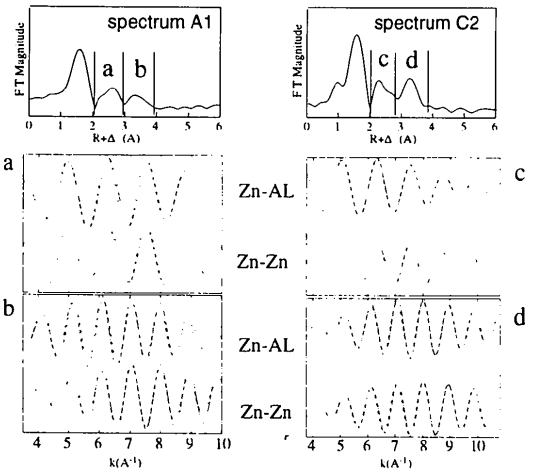

Figure 2. Comparison of the second and third shells fits for two representative spectra. The fits (solid) are of the filtered shells (dashed) as indicated. In panels a and c Al gives the best fit for the second shell. In panels b and d both Al and Zn give reasonable fits. a. Zn-Al: N=4.0, R=3.09Å, Zn-Zn: N=1.4, R=3.25Å. b. Zn-Al: N=2.4 and 2.4, R=3.72 and 4.06Å, Zn-Zn: N=1.8, R=3.84Å. c. Zn-Al: N=5.5, R=3.05Å, Zn-Zn: N=2.6, R=3.20Å. d. Zn-Al: N=8.8, R=4.06Å, Zn-Zn: N=4.2, R=3.80 Å. σ^2 was held fixed in all fits at 0.01Å^2.

a single shell was used, and the Zn-O distances and coordination numbers reported in Table 1 are an average of the aqueous and sorbed components. The *in-situ* spectra give similar distances for the second-shell Al (2.97-3.14Å) compared to the *ex-situ* samples. An additional Al shell was included in the fits of the *in-situ* horizontal spectra (B1 and E1) which gives a distance of ~3.5Å in both cases. More distant Al (or Zn) shells are not observed. The change in the Zn-O distance and lack of more distant shells of Al (or Zn) indicate that the sorbtion complex is altered upon removal of the sample from bulk solution.

4. Summary and Conclusions

Zn(II) is bound in an inner-sphere manner on α-Al_2O_3 (0001) and (1-102) single crystal surfaces. For all spectra an Al shell was fit in the range of 2.9-3.1Å consistent with bidentate linkage of Zn(II) to an AlO_6 octahedron. In our recent work on Zn(II) sorption on α-Al_2O_3 powders (Thompson et al., 1998; Trainor and Brown, 1997) we found a similiar Zn-Al distance of roughly 2.96Å at low sorption densities (Γ< 1.5μmoles/m^2). Further, the low coverage powder results indicated that that zinc binds in four-fold coordination with nearest neighbor oxygen having a Zn-O distance of 1.96Å, similiar to our *in-situ* results presented here. However, in the powder samples there is no evidence for more distant Al shells at low coverage, while at higher surface coverages we find a Zn-Al co-precipitate with a hydrotalcite type structure (Fig 3, (ii)). These mixed Me(II)/Al(III) phases have been found previously for Zn(II)/γ-Al_2O_3 (d'Espinose et al., 1995) and for other Me(II)/alumina systems (Towle et al., 1997; Scheidigger et al., 1997; Thompson et al., 1999). We find no evidence of the formation of the mixed Zn(II)/Al(III) hydrotalcite type phases on the single crystals under the conditions examined in this study.

Results for the (0001) and (1-102) sample orientations are similar even though the idealized surface structure of the two cuts is significantly different. The polarization dependence of the *ex-situ* samples and similiarity of results from the two cuts

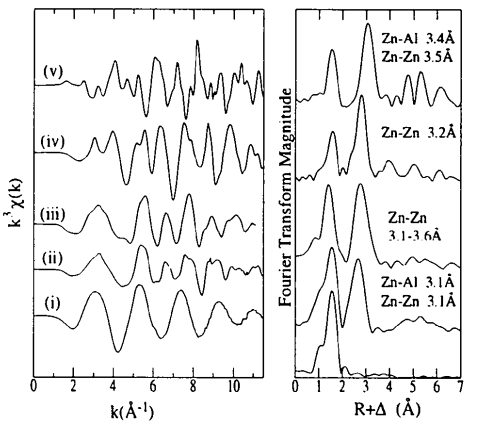

Figure 3. Model compound EXAFS and Fourier transforms. (scaled for visualization). (i) 10mM, pH3.6 $Zn(NO_3)_2$ solution, (ii) Zn/Al co-precipitate, (iii) $Zn_5(NO_3)_2(OH)_8.2H_2O$, (iv) ZnO, (v) $ZnAl_2O_4$

leads us to postulate one model in which sorption is predominantly occuring at steps which may be more prevelent on the (0001) surface. However, the results indicate that the average Zn-O bond length for the *in-situ* samples is shorter than the *ex-situ* samples and the *in-situ* samples lack of the more distant shell in the horizontal orientation. The lack of the strong third shell in the horizontal spectra and the change in the first-shell Zn-O distances of the *in-situ* spectra indicate that the sorption complex is altered in the absence of bulk solution. Therefore, formation of zinc clusters or polymer chains upon removal of the bulk solution cannot be ruled out. Additional work, including further characterization of the surface topography and more detailed analysis of possible sorption geometries are required to distinguish between these models.

Acknowledgments

We would like to thank the SSRL staff for help with XAS experiments. This work was funded by DOE Grant DE-FG03-93ER14347-A006.

References

Baes, C.F. and Mesmer, R.E. (1976). *The Hydrolysis of Cations*, pp 287-294. New York: John Wiley and Sons.

Citrin, P.H. (1985). *Phys. Rev. B* **31**, 700-721.

d'Espinose de la Caillerie, J. B., Bobin, C., Rebours, B., and Clause, O. (1995). *Stud. Surf. Sci. Catal.* **91**, 169-84.

Effenberger, H., Mereiter, K. and Zeman, J. (1981). Zeitschrift für Kristallographie **156**, 233-243.

George G.N. and Pickering I.J. (1995). EXAFSPAK, Stanford Synchrotron Radiation Laboratory.

Munoz-Paez, A., Pappalardo, R. R., and Marcos, E. S. (1995). *J. Am. Chem. Soc.* **117**, 11710-11720.

Rehr, J.J., Mustre de Leon, J.,Zabinsky, S.I., and Albers, R.C. (1991). *J. Am. Chem. Soc.* **113**, 5135.

Ressler, T., Brock, S.L., Wong, J. and Suib, S.L. (1998). *J. Phys. Chem.* Submitted.

Scheidegger, A. M., Lamble, G. M., and Sparks, D. L. (1997). *J. Coll. Int. Sci.* **186**, 118-128.

Thompson, H.A., Fitts, J.P., Trainor, T.P., Parks, G.A. and Brown, G. E. Jr. (1998). *1997 Activity Report, Stanford Synchrotron Radiation Laboratory*, 7-181.

Thompson, H.A., Parks, G.A., and Brown, G.E. Jr. (1999). *Clays and Clay Minerals*. In Press

Towle, S. N., Bargar, J. R., Brown, G. E., and Parks, G. A. (1997). *J. Coll. Int. Sci.* **187**, 62-82.

Trainor, T.P. and Brown, G.E., Jr. (1997). *EOS Transactions* **78**, F768.

(Received 10 August 1998; accepted 9 December 1998)